High Affinity, Stability, and Lactonase Activity of Serum Paraoxonase PON1 Anchored on HDL with ApoA-I†

Leonid Gaidukov and Dan S. Tawfik*

Department of Biological Chemistry, Weizmann Institute of Science, Rehovot 76100, Israel

Received May 10, 2005; Revised Manuscript Received June 15, 2005

ABSTRACT: Serum paraoxonase (PON1) is a high-density lipoprotein (HDL)-associated enzyme exhibiting antiatherogenic properties. This study examined the interaction of recombinant PON1 with reconstituted HDL comprised of PC, cholesterol, and various apolipoproteins (apoA-I, -II, and -IV). The affinity, stability, and lactonase activity were strongly correlated, with apoA-I exhibiting the strongest effects, apoA-IV exhibiting weaker yet significant effects, and apoA-II having a negative effect relative to protein-free particles. We found that PON1 binds apoA-I HDL with sub-nanomolar affinities ($K_d \ll 10^{-9}$ M) and slow dissociation rates ($t_{1/2} > 80$ min), while binding affinity for other particles was dramatically lower. A truncated form of PON1 lacking the N-terminal helix maintains considerable binding to apoA-I HDL ($K_d = 1.2 \times 10^{-7}$ M), validating the structural model which indicates additional parts of the enzyme involved in HDL binding. Kinetic inactivation assays revealed the existence of an equilibrium between two forms of PON1 differing in their stability by a factor of 100. Various lipoproteins and detergent preparations shift this equilibrium toward the more stable conformation. Consistent with its highest affinity, only apoA-I HDL is capable of totally shifting the equilibrium toward the stable form. The paraoxonase and arylesterase activities were stimulated by HDL by 2−5-fold as previously reported, almost independently of the apoliporotein content. In contrast, only apoA-I is capable of stimulating the lactonase activity by ≤20-fold to k_{cat}/K_M values of 10^6-10^7 M^{-1} s^{-1}, while apoA-IV and apoA-II have almost no effect. Overall, the results indicate the high stability, selectivity, and catalytic proficiency of PON1 when anchored onto apoA-I HDL, toward lactone substrates, and lipophilic lactones in particular.

Serum paraoxonase (PON1)[1] belongs to a family of enzymes that catalyze the hydrolysis of a broad range of carboxy esters, carbonates, and lactones, as well as toxic organophosphates, including the insecticide paraoxon (*1*, *2*). An emerging body of evidence indicates that PON1 possesses important antiatherogenic roles. Human serum PON1 levels and catalytic proficiencies are inversely proportional to the risk of coronary heart disease (*3*, *4*), and PON1 knockout mice are highly susceptible to atherosclerosis (*5*). PON1 is known to reside on the high-density lipoprotein (HDL) cholesterol-carrying particles, which play a key role in neutralizing potentially toxic, hydrophobic components of plasma, including oxidized lipids (*6*). The PON1−HDL complex is thought to protect against oxidative modifications, mediate the efflux of cholesterol from macrophages, and reduce the level of oxidized lipid forms involved in the development of atherosclerosis (*7*−*9*).

The endogenous substrate(s) and mechanism of the antiatherogenic activity of PON1 remain largely unknown. It is becoming apparent, however, that despite its traditional assignment as paraoxonase/arylesterase, PON1 is in fact a lactonase. PON1 has been shown to catalyze the hydrolysis of a variety of lactones (*2*, *10*), as well as lactone formation (*11*). Moreover, laboratory evolution (*12*) and structure−reactivity studies of PON1 (*13*) indicated that PON1 is primarily a lactonase. In fact, the lactonase activity is the only activity common to all members of the PON family, and directed evolution of PON1 has led to PON1 variants with activity patterns and active site residues that resemble those of PON2 or PON3 (i.e., high lactonase/esterase activity and very low paraoxonase activity) (*12*, *14*). Thus, lactones derived from fatty acid oxidation products may comprise the native substrates of PON1 (*10*, *15*).

PON1 is synthesized in the liver and secreted into the blood where it is associated with HDL-type complexes (*16*, *17*). PON1's localization on HDL seems to be critically important for its activity in vivo, probably by stabilizing the enzyme and providing an optimal environment for the interaction with its physiological substrates. PON1 can also associate with other amphiphilic complexes such as phospholipid and detergent micelles (*18*−*20*). PON1's hydrophobic N-terminus is compatible with a transmembrane helix (dubbed H1), and was suggested to mediate the anchoring of PON1 to HDL and phospholipid micelles (*14*, *18*, *21*). The crystal structure of a PON1 indicated an adjacent

† This work was supported by the Benoziyo Institute of Molecular Medicine. D.S.T. is the incumbent of the Elaine Blond Career Development Chair.

* To whom correspondence should be addressed. Phone: +972 8 934 3637. Fax: +972 8 934 4118. E-mail: tawfik@weizmann.ac.il.

[1] Abbreviations: PON1, serum paraoxonase; rePON1, recombinant PON1; HDL, high-density lipoprotein; rHDL, reconstituted HDL; Apo, apolipoprotein; PC, egg L-α-phosphatidylcholine; FC, free (unesterified) cholesterol; DPPE, dipalmitoylphosphatidylethanolamine; SPR, surface plasmon resonance; RU, resonance units; SUV, small unilamellar vesicles; 5-HETEL, 5(*S*)-hydroxy-6(*E*,*Z*),11(*Z*),14(*Z*)-eicosatetraenoic acid, 1,5-lactone; LCAT, lecithin cholesterol acyltransferase.

10.1021/bi050862i CCC: $30.25
Published on Web 08/16/2005

amphipathic helix, H2 (*14*). The two helices form hydrophobic patches that are found in the marked proximity of the active site of PON1 and provide a potential surface for interaction with the lipid layer of HDL. The structural model implies that HDL anchoring modifies PON1's active site and significantly alters its enzymatic properties, yet the enzymology and substrate specificity of PON1 in its native environment, namely, on HDL particles, with the relevant lipid and lipoprotein content, have not been thoroughly examined.

HDL constitutes a group of particles comprised of membrane components, such as phospholipids, cholesterol, and cholesterol esters, as well as protein components (*22*). Apolipoprotein A-I (apoA-I) is the major structural protein on HDL, and it plays a critical role in determining the structure and composition of HDL particles (*23*, *24*). Two major apoA-I-containing HDL particles exist: Lp AI+AII, composed of both apoA-I and apoA-II, and Lp A-I, which contains only apoA-I (*22*, *25*). Other, minor HDL particles contain lipoproteins apoA-IV, apoCs, and apoE (*22*). Several lines of evidence demonstrate the preferential association of PON1 with apoA-I-containing HDL particles in vivo and in vitro (*26*, *27*). PON1 copurifies with apoA-I (*28*), and immunoassays of sera show that PON1 is mainly found in association with apoA-I HDL particles (*29*). Finally, both native and reconstituted HDL particles carrying apoA-I promote the release of human PON1 from cells, stabilize the enzyme, and increase its arylesterase activity (*18*, *19*, *27*).

The goal of this study was to investigate the details of PON1's interaction with HDL particles carrying different apolipoproteins, and the enzymology of the HDL-anchored PON1. Interference by copurified serum components has repeatedly complicated the study of PON1 (*10*, *30*−*32*). We therefore developed a reconstituted in vitro system based entirely on purified lipid components and recombinant proteins expressed in *Escherichia coli*. We examined a recombinant PON1 analogue (rePON1) that is almost identical to rabbit PON1 (*12*, *33*), and its truncated variant lacking the first 20 amino acids corresponding to the hydrophobic N-terminus (Δ20-rePON1). We applied these PON1 variants onto reconstituted HDL particles (rHDL) composed of PC, cholesterol, and apoA-I, apoA-II, apoA-IV, or no lipoprotein. We determined the binding affinity, stability, and a range of enzymatic activities for the various PON1−HDL combinations. Our results indicate a unique behavior of apoA-I particles: these exhibit the highest affinity for PON1 ($>10^9$ M^{-1}) and shift PON1 toward a single, highly stable conformation that exhibits high catalytic efficiency and selectivity toward lactone substrates.

MATERIALS AND METHODS

Production of rePON1s. rePON1-G3C9 was used to generate the intact (rePON1) and truncated (Δ20-rePON1) proteins as described previously (*12*, *33*) with the following variations. Briefly, the rePON1-G3C9 gene fused to a His_8 tag directly at its carboxy terminus was cloned at *Nco*I−*Not*I restriction sites into the pET32b vector (Novagen), from which the Trx fusion protein and peptide tags had been truncated (pET32-trx) (*33*). Δ20-rePON1 was constructed from the rePON1-G3C9-His_8 gene by PCR amplification with a primer that introduced an *Nco*I site (encoding Met-Ala) at the 5′ end of the gene encoding Gln20, and recloned into pET32-trx. Competent origamiB (DE-3, Novagen) cells were transformed with the plasmids and grown for 48 h (8 h at 30 °C and then 40 h at 20 °C) in 2×TY medium, supplemented with 1 mM $CaCl_2$, 100 μg/mL ampicillin, and 30 μg/mL kanamycin. Cells were harvested by centrifugation, resuspended, and disrupted by sonication to obtain cleared lysate, to which ammonium sulfate was added (55% wt/vol). Precipitated proteins were purified on a Ni−NTA column (Qiagen). Fractions were analyzed for paraoxonase activity and purity (by SDS−PAGE), pooled, dialyzed against storage buffer [50 mM Tris (pH 8.0), 50 mM NaCl, 1 mM $CaCl_2$, and 0.1% tergitol], supplemented with 0.02% sodium azide, and stored at 4 °C.

Production of Recombinant Apolipoproteins. The human apoA-I gene in the pET20b vector, containing an N-terminal Met-Ala-$(His)_6$-Ser-Gly tag (*27*), was kindly provided by M. Oda (Oakland Research Institute, Oakland, CA). Rabbit apoA-I was amplified from cDNA prepared from fresh liver of New Zealand rabbits, and modified by PCR with a 5′ oligo appending an N-terminal Met-Arg-Gly-Ser-$(His)_6$-Ser-Gly tag. The resulting fragment was cloned into the pET20b vector (Novagen) using the *Nde*I−*Nco*I restriction sites. Both ApoA-Is were purified essentially as described previously (*27*) with slight variations. Briefly, the plasmids described above were transformed into BL21(DE3) pLysS cells (Novagen). Cells were grown to an OD_{600} of 0.6 in 2×TY medium supplemented with 100 μg/mL ampicillin, induced with 0.4 mM IPTG, and cultured overnight at 25 °C. The cells were harvested by centrifugation, resuspended in PBS [10 mM Na_2HPO_4 (pH 7.3) and 150 mM NaCl] supplemented with 1 mM DTT and 10 μL of protease inhibitor cocktail (Sigma), and lysed by sonication. Cleared lysates were supplemented with 3 M guanidine hydrochloride and purified to homogeneity on a Ni−NTA column. Purified proteins were dialyzed extensively against Tris-buffered saline (TBS) [10 mM Tris (pH 8.0) and 150 mM NaCl], supplemented with 0.1 mM EDTA and 0.02% sodium azide, and stored at 4 °C. Given that our rePON1 variants are most homologous to rabbit PON1, rabbit apoA-I rHDL was routinely used throughout the study, although rHDL containing human apoA-I gave essentially identical results in all the assays that were tested. The apoA-II gene was amplified from human liver cDNA (Clontech) and cloned into the pET32b vector for expression as fusion protein with thioredoxin (Trx) and a His_6 tag. The plasmid was transformed into BL21(DE3) pLysS cells that were then grown to an OD_{600} of 0.6 in 2×TY medium supplemented with 100 μg/mL ampicillin, induced with 1 mM IPTG, and cultured for 3 h at 30 °C. The apoA-II was then purified as described above for apoA-I. The fusion tags were removed by proteolytic digestion using recombinant enterokinase (Novagen), and the intact apoA-II was separated from the fusion tags by Ni−NTA chromatography, dialyzed against TBS, supplemented with 0.1 mM EDTA and 0.02% sodium azide, and stored at 4 °C. The human apoA-IV gene in the pET30 vector was kindly provided by K. Pearson and S. Davidson (University of Cincinnati, Cincinnati, OH). The protein was expressed and purified as described previously (*34*).

Preparation of rHDL and Small Unilamellar Vesicles (SUV). Discoidal rHDL containing apoA-I, apoA-II, or apoA-IV was prepared by the cholate dialysis method (*35*, *36*).

Briefly, egg L-α-phosphatidylcholine (PC; Avanti Polar Lipids), free cholesterol (FC; Sigma), and apolipoproteins were combined at a molar ratio of 100/5/1, suspended with sodium deoxycholate (Sigma) at a cholate/PC molar ratio of 2/1, and dialyzed extensively against TBS to remove all sodium cholate. PC/FC particles were prepared by the same procedure with no protein components. For Biacore studies, 0.7% of *N*-biotinyl-dipalmitoylphosphatidylethanolamine (*N*-biotynyl-DPPE; Avanti Polar Lipids) was added to the bulk mixture of egg PC and FC during reconstitution, resulting in an average ratio of 1.4 biotins per rHDL particle (*37*). Phospholipid particles were isolated by ultracentrifugation in a KBr density gradient as described previously (*27*). Fractions containing the highest lipid and protein content were pooled, dialyzed against TBS, and stored at 4 °C. The phospholipid content of rHDL was determined by the enzymatic method (Sentinel) and protein content using the BCA kit (Pierce). The concentration of rHDL was determined on the basis of the apolipoprotein concentration, assuming an apoA/rHDL ratio of 2/1 (*35*, *36*). The homogeneity of the preparations was assessed by nondenaturing gradient gel electrophoresis (4 to 20% polyacrylamide, Pharmacia) indicating the formation of ~10 nm particles (*35*, *36*). Small unilamellar vesicles were prepared by sonication of a dispersion of egg PC, FC, and *N*-biotynyl-DPPE at a molar ratio of 100/5/0.1 in TBS buffer.

Surface Plasmon Resonance (SPR). SPR was performed on a BIAcore 3000 instrument (BIAcore, Uppsala, Sweden). The streptavidin (SA5) chip (a carboxymethyldextran hydrogel derivatized with streptavidin) was used to adsorb the biotinylated particles described above. Typically, rHDL (20 μg/mL apolipoproteins) or SUV (0.4 mg/mL PC) were injected over the chip surface at a flow rate of 10 μL/min in running buffer (TBS supplemented with 1 mM $CaCl_2$) until 500−1000 resonance units (RU) of the biotinylated particles were immobilized. The binding assay was performed by injecting rePON1 solutions in running buffer at 10 different concentrations (typically, 0.02−0.2 μM for apoA-I, apoA-IV rHDLs, and SUV and 0.2−2 μM for apoA-II rHDL) at a flow rate of 20 μL/min at 25 °C. These conditions resulted in a linear relation between the protein concentration and the maximal (steady-state) response, indicating the pseudo-first-order regime in relation to the immobilized particles. Injections were performed simultaneously over the immobilized and blank surface (containing streptavidin only with no immobilized particles), and the net signal was obtained by subtracting the blank signal from the signal of the immobilized surface. The association phase for the intact rePON1 binding to all types of particles was followed for 7 min, and the dissociation phase was monitored for 30 min; for Δ20-rePON1, the association and dissociation phases were monitored for 4 min. Surface regeneration between consecutive binding cycles included a 2 min injection of 1 M NaCl with 3 mM NaOH.

SPR Data Analysis. The binding rate constants were obtained by fitting of association and dissociation phases to single exponentials, assuming a first-order (dissociation) or a pseudo-first-order (association) regime based on a large (≥10-fold) excess of the immobilized particles relative to rePON1. The following equations were used to fit the association and dissociation curves, respectively: $R_t = R - A \exp(-k_{on}^{obs} t)$, $R_t = R + A \exp(-k_{off} t)$, where R_t is the response in RU at time t that corresponds to the concentration of the molecular complex formed, R is the final response at infinite time, A is a correlation coefficient, k_{on}^{obs} is the observed association rate constant at a given rePON1 concentration, and k_{off} is the dissociation rate constant. The association rate constant, k_{on}, was derived from the linear fit of k_{on}^{obs} versus concentration ($k_{on}^{obs} = [\text{rePON1}]k_{on} + k_{off}$). The k_{off} value derived from this fit was essentially identical (within the error range) to the value derived directly from the dissociation phase. The equilibrium binding constant, K_d, was obtained from the ratio of the rate constants (k_{off}/k_{on}). Data fitting was performed with KaleidaGraph 5.0.

Stability Studies. Samples of rePON1 in storage buffer were thoroughly delipidated using Bio-Beads SM-2 (Bio-Rad) taken in excess (typically, incubation for 4 h of a 100 μL protein sample with 20 mg of washed beads), diluted to 0.2 μM in activity buffer [50 mM Tris (pH 8.0) and 1 mM $CaCl_2$], and preincubated for 30 min at 37 °C with a large excess of rHDLs (10 μM) or 0.1% tergitol (NP-10, Sigma; 15 μM detergent micelles) in activity buffer. Inactivation was initiated by adding an equal volume of inactivation buffer [10 mM EDTA and 20 mM β-mercaptoethanol in 50 mM Tris (pH 8.0)] and incubating the samples at 37 °C. Aliquots were taken at certain time points and diluted in activity buffer, and the residual activity was determined with 1 mM phenyl acetate as described previously (*33*). Inactivation rates were fitted to either mono- or double-exponential fits: $R = A_1 \exp(-k_1^{inact} t) + A_2 \exp(-k_2^{inact} t)$, where R is the residual activity (expressed as the percentage of the initial activity of the delipidated enzyme), A is the amplitude of each of the single-exponential phases, and k is the rate constant of inactivation for that phase. Subscripts 1 and 2 designate the first (fast) and second (slow) phases of inactivation, respectively.

Stimulation of PON1 Activity by rHDL. Delipidated rePONs were diluted to 0.2 μM in activity buffer and incubated with a range of rHDL concentrations (0.1−10 μM) for 2−4 h at 37 °C. Enzymatic activity was detected with various substrates at 1 mM.

Enzyme Kinetics. Enzymatic parameters with phenyl acetate and paraoxon were determined by Michaelis−Menten analysis as described previously (*12*, *33*). Enzyme kinetics with δ-valerolactone and γ-dodecanoic lactone were performed by the pH-sensitive colorimetric assay as described previously (*13*) with slight variations. Briefly, rePON1s were diluted in Bicine buffer [2.5 mM Bicine (pH 8.3), 0.2 M NaCl, and 1 mM $CaCl_2$] in the presence of 0.2−0.3 mM Cresol Purple indicator. A range of substrate concentrations was prepared in Bicine buffer with 1−2% DMSO in all reactions (Triton detergent was not added to γ-dodecanoic lactone preparations), and proton release by the carboxylic acid product was monitored spectrophotometrically at 577 nm. The initial rates of product formation (V_0) were derived from a standard calibration curve obtained with acetic acid, and when necessary, rates of spontaneous hydrolysis of the lactones in buffer were subtracted from enzymatic rates. The kinetic parameters were determined by Michaelis−Menten analysis of initial rates [$v_0 = k_{cat}[E]_0[S]_0/([S]_0 + K_M)$]. Lactonase activity assays with 5(*S*)-hydroxy-6(*E*,*Z*),11(*Z*), 14(*Z*)-eicosatetraenoic acid, 1,5-lactone (5-HETEL; Cayman) were performed essentially as described previously (*11*) with the following variations. 5-HETEL (1 mM in acetonitrile)

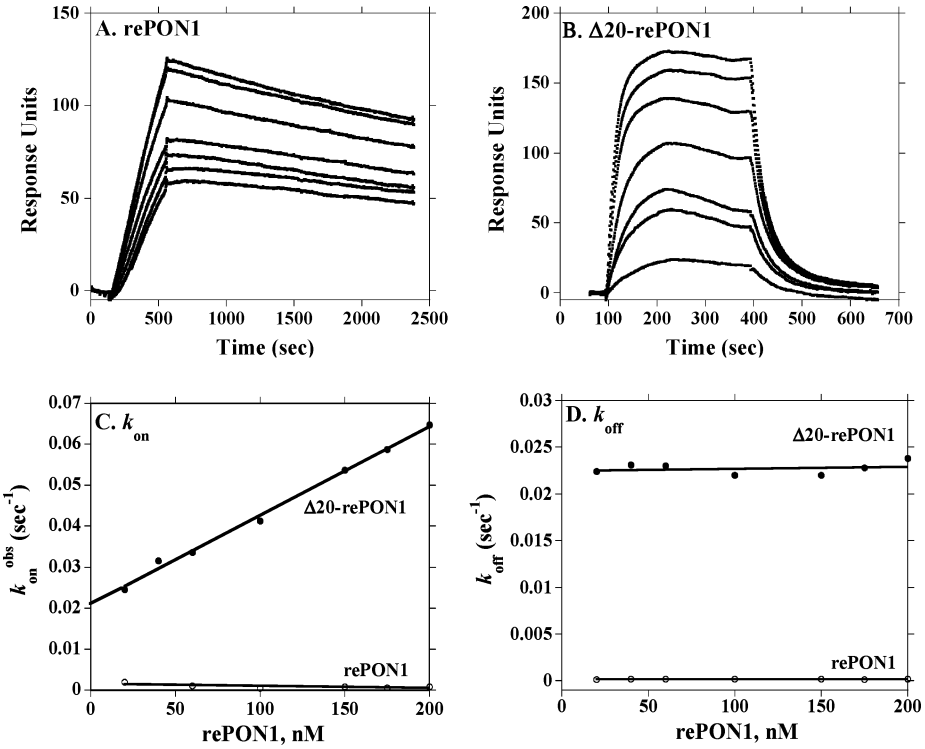

FIGURE 1: SPR sensorgrams of the binding of various concentrations of rePON1 (A) and Δ20-rePON1 (B) to apoA-I rHDL. Biotinylated apoA-I rHDL particles were immobilized onto the streptavidin surface (SA chip), and a series of PON1 concentrations were injected over the immobilized particles and a blank surface to obtain the net binding response. Binding was performed at 25 °C in TBS buffer. Association and dissociation phases were fitted to a single exponential to give k_{on}^{obs}. k_{on} was derived from the linear fit of k_{on}^{obs} vs concentration ($k_{on}^{obs} = [\text{rePON1}]k_{on} + k_{off}$) (C). k_{off} was derived directly from k_{off}^{obs} that was independent of PON1 concentration (D). Concentrations of both proteins are (from bottom to top) 20, 40, 60, 100, 150, 175, and 200 nM.

was dissolved at 10−20 μM in reaction buffer [50 mM Tris (pH 7.5) and 1 mM $CaCl_2$] with 2% acetonitrile, and incubated with 0.004−0.05 μg/mL rePON1 samples at room temperature for 1 min. Reactions were stopped by adding an equal volume of acetonitrile with 0.2% acetic acid, and analyzed by reverse-phase HPLC (Amersham Biosciences) on an analytical C18 column (250 mm × 4.6 mm, 5 μm particles; Vydac) using a 65 to 80% linear gradient of acetonitrile in water (1%/min), both solvents containing 0.2% acetic acid. Quantification of the extent of hydrolysis was based on the ratio of peak areas of hydroxy acid (elution at 7.3 min) and lactone (elution at 15.2 min) detected at 236 nm. Data were fitted to the linear regime of the Michaelis−Menten model [$v_0 = [S]_0[E]_0k_{cat}/K_M$], and k_{cat}/K_M was deduced from the slope.

RESULTS

Affinity Measurements. Binding affinities of rePON1, and its truncated variant (Δ20-rePON1), for HDL particles with various apolipoprotein compositions were determined by surface plasmon resonance. Reconstituted particles containing no apoA (PC/cholesterol vesicles), apoA-I, apoA-II, or apoA-IV and a small amount (0.7%) of biotinylated lipids were generated (*37*), and immobilized onto the surface of the streptavidin sensor chip. Biotinylation resulted in an average of ∼1.4 biotin molecules per rHDL particle, and had no measurable effect on the properties of these particles with regard to stabilization and stimulation of PON1's activity (see below). PON1 samples were freshly delipidated from detergent, diluted in buffer, and injected in a series of concentrations over immobilized rHDL particles and a blank reference surface (streptavidin only). Typical binding sensorgrams for the interaction with apoA-I particles are portrayed in panels A and B of Figure 1. The association and dissociation rate constants were obtained by fitting of the association and dissociation phases to a single exponential, assuming a first-order (dissociation) or pseudo-first-order reaction (association at [rHDL] ≥ 10[PON1]). The resulting rate and affinity constants are given in Table 1.

The truncated analogue exhibited a linear dependency of association rates and Δ20-rePON1 concentration (Figure 1C), while the dissociation of Δ20-rePON1 was concentration-independent and was completed within 4 min (Figure 1B,D). The derived association rate constant for Δ20-rePON1 and apoA-I rHDL is 2×10^5 s^{-1} M^{-1}, and the dissociation rate is 2.3×10^{-2} s^{-1}, yielding an equilibrium dissociation constant, K_d, of 1.2×10^{-7} M. In contrast, the association of the intact rePON1 with the apoA-I particles exhibited a nonregular behavior: the association rates were constant throughout the range of PON1 concentrations ($k_{on}^{obs} \approx 1.7 \times 10^{-3}$ s^{-1}; Figure 1C) indicating a zero-order, rate-limiting step that occurs prior to the association of PON1 with the HDL particles. In detergent solutions, PON1 coexists in a variety of forms, including dimers and oligomeric forms, while the monomeric form appears in solutions containing a large excess of detergent micelles (*20*). We assume that the rate-limiting step may involve the dissociation of the protein from any of these forms (most likely dimers and higher-order lipid−protein complexes, given that the sample was delipidated which minimized the amount of detergent but did not eliminate it) into another form that can associate with HDL. This step appears to be much slower than the

Table 1: Kinetic and Affinity Constants for the Binding of rePON1 and Δ20-rePON1 to HDL Particles

	rePON1			Δ20-rePON1		
surface	k_{on}^{obs} (s^{-1})[b]	k_{off} (s^{-1})	K_d (M)[d]	k_{on} (s^{-1} M^{-1})	k_{off} (s^{-1})	K_d (M)
apoA-I rHDL[a]	$(1.7 \pm 0.7) \times 10^{-3}$	$(1.5 \pm 0.4) \times 10^{-4}$ [c]	$<0.75 \times 10^{-9}$	$(2.0 \pm 0.3) \times 10^{5}$	$(2.3 \pm 0.1) \times 10^{-2}$	$(1.2 \pm 0.2) \times 10^{-7}$
apoA-II rHDL[a]	$(2.1 \pm 0.6) \times 10^{-3}$	$(6.2 \pm 1.2) \times 10^{-4}$	$\leq 4.4 \times 10^{-8}$	$(1.4 \pm 0.3) \times 10^{4}$	$(2.5 \pm 0.3) \times 10^{-2}$	$(1.8 \pm 0.8) \times 10^{-6}$
apoA-IV rHDL[a]	$(1.5 \pm 0.6) \times 10^{-3}$	$(2.3 \pm 0.7) \times 10^{-4}$	$\leq 1.3 \times 10^{-9}$	$(1.8 \pm 0.5) \times 10^{5}$	$(2.8 \pm 0.3) \times 10^{-2}$	$(1.6 \pm 0.2) \times 10^{-7}$
PC/FC vesicles[a]	$(2.7 \pm 0.3) \times 10^{-3}$	$(5.5 \pm 0.9) \times 10^{-4}$	$\leq 3.2 \times 10^{-9}$	$(1.7 \pm 0.4) \times 10^{5}$	$(1.0 \pm 0.2) \times 10^{-2}$	$(5.9 \pm 0.2) \times 10^{-8}$

[a] Reconstituted HDL particles were prepared by cholate dialysis and contained egg PC, FC, *N*-biotynyl-DPPE, and apoA-I, apoA-II, or apoA-IV. PC/FC vesicles were prepared by sonication and contained egg PC, FC, and *N*-biotynyl-DPPE. Binding experiments were performed at 25 °C. Each value represents the mean ± the standard deviation of two independent experiments. [b] Observed association rate constants (k_{on}^{obs}) are presented instead of the association rate constants (k_{on}), since the association rates for rePON1 binding to all types of particles were not dependent on the concentration (probably due to protein oligomerization) and, therefore, could not be determined. Association rate constants for Δ20-rePON1 were derived from the linear fit of k_{on}^{obs} vs concentration ($k_{on}^{obs} = [\Delta 20\text{-rePON1}]k_{on} + k_{off}$). [c] The dissociation rate (k_{off}) for rePON1 binding to apoA-I rHDL might be significantly lower than the constant presented here, since it was enhanced by the slow baseline drift that occurred during the experiment. [d] Affinity constants for rePON1 represent the upper limit of K_d, and were derived assuming that the association rates (k_{on}) are equal to the respective association rates of Δ20-rePON1.

association itself and hence dictates the rate. This interpretation is also supported by the fact that the essentially same k_{on}^{obs} value ($\sim 2 \times 10^{-3}$ s^{-1}; Table 1) was observed with all HDL particles regardless of their lipoprotein components. The dissociation of rePON1 from apoA-I particles was extremely slow (half-life of ≤80 min), and had to be monitored for 30 min to detect a minimal dissociation amplitude. However, the observed dissociation rate undoubtedly contains a component of baseline drift due to the decomposition or detachment of the HDL particles from the surface. Indeed, the rate of this drift (as observed prior to PON1 loading) is comparable to the rate of dissociation. Thus, the actual rate of dissociation of rePON1 from apoA-I HDL is definitely slower than the dissociation rate constant calculated from these data (1.5×10^{-4} s^{-1}; Table 1). Likewise, assuming that the association rate (k_{on}) of the intact PON1 is the same as for Δ20-rePON1, we can state an upper limit for the equilibrium dissociation constant, K_d, of 0.75×10^{-9} M. However, the actual K_d is probably significantly lower since the k_{on} value of the intact enzyme is likely to be higher than that of the truncated form ($>2 \times 10^{5}$ s^{-1} M^{-1}), and the k_{off} is probably lower than 1.5×10^{-4} s^{-1}.

Binding of PON1 to apoA-II rHDL was much weaker compared to binding to apoA-I rHDL, and 10-fold higher concentrations of the proteins were required (data not shown). As for apoA-I particles, the association rate of rePON1 with apoA-II rHDL was not concentration-dependent ($k_{on}^{obs} = 2.1 \times 10^{-3}$ s^{-1}), while the dissociation rate was clearly visible and much faster than the baseline drift ($k_{off} = 6.2 \times 10^{-4}$ s^{-1}). The binding affinity of the truncated Δ20-rePON1 for apoA-II HDL was 15-fold lower than for apoA-I particles ($K_d = 1.8 \times 10^{-6}$ M; Table 1), mainly due to the decrease in the association rate. In contrast to the significantly reduced affinities for apoA-II particles, PONs binding to apoA-IV rHDL showed values similar to those of apoA-I particles (Table 1). The rate of dissociation of rePON1 from apoA-IV rHDL (2.3×10^{-4} s^{-1}) was faster than the baseline drift, and slightly higher than that observed with apoA-I rHDL. Finally, PC/FC vesicles devoid of any apolipoprotein exhibited a 4-fold faster dissociation rate with rePON1 than the apoA-I particles, while Δ20-rePON1 showed, instead, a 2-fold lower dissociation rate (1.0×10^{-2} s^{-1}) and an affinity constant of 5.9×10^{-8} M (Table 1).

In summary, rePON1 exhibited very slow dissociation rates, and affinities in the low nanomolar range. The truncated variant (Δ20-rePON1) exhibits ca. 100-fold higher dissociation rates than the intact protein, and lower affinities in accordance, although its K_d value is still relatively high ($\sim 10^{-7}$ M with apoA-I rHDL). Although the lipid component of HDL seems to drive PON1's binding to a large extent (the K_d for PC/FC particles is $\leq 3.2 \times 10^{-9}$ M), the protein component plays a significant role: the lowest dissociation rates and highest affinities are observed with apoA-I ($K_d < 10^{-9}$ M), and then with apoA-IV, while apoA-II seems to disrupt the interaction (K_d ca. 15-fold lower than with protein-free PC/FC vesicles).

Stability Measurements. To analyze the effect of HDL on the stability of PON1, we examined the progress of the enzyme's inactivation in the presence of a large (50-fold) excess of different HDL particles. Delipidated rePON1 and Δ20-rePON1 samples in buffer, 0.1% tergitol, or rHDL mixtures composed of either apoA-I, apoA-II, apoA-IV, or PC and FC only were incubated at 37 °C in the presence of a calcium chelator (EDTA) and the reducing agent β-mercaptoethanol (*38*). The rate of inactivation was monitored by measuring the residual arylesterase activity at different time points, and comparing it to the initial activity of the delipidated enzyme (designated as 100%). Representative inactivation profiles for rePON1 and Δ20-rePON1 are presented in panels A and B of Figure 2, respectively, and the derived inactivation rate constants are summarized in Table 2. Incubation of the delipidated rePON1 with apoA-I rHDL resulted in an immediate 4.2-fold increase in the arylesterase activity of the enzyme, as previously observed with serum-purified human PON1 (*18*, *19*). A slow inactivation followed, obeying, as expected for a unimolecular process, an exponential curve with an amplitude (*A*) of 420% and a rate constant ($k^{inactiv}$) of 0.01 s^{-1}, corresponding to a half-life ($t_{1/2}^{inactiv}$) of ~70 h. Since the inactivation kinetics followed a single phase, the obtained amplitude constitutes a full fraction (1.0) of the total amplitude of the reaction (Table 2). In contrast, the inactivation kinetics of all other preparations of rePON1 followed a double-exponential regime (Figure 2A), indicating the presence of two enzyme forms. One form is highly unstable and undergoes fast inactivation: $k_1^{inactiv}$ for apoA-IV and PC/FC is ~ 1 h^{-1} (Table 2), while the other form is 100 times more stable and exhibits an inactivation rate that is very similar to that of the apoA-I rHDL-anchored PON1 ($k_2^{inactiv} = 0.01$ s^{-1}). The difference between these particles (PC/FC, apoA-I, and apoA-IV) is therefore in the partition between the two phases, or enzyme forms, although the rates of inactivation are strikingly similar.

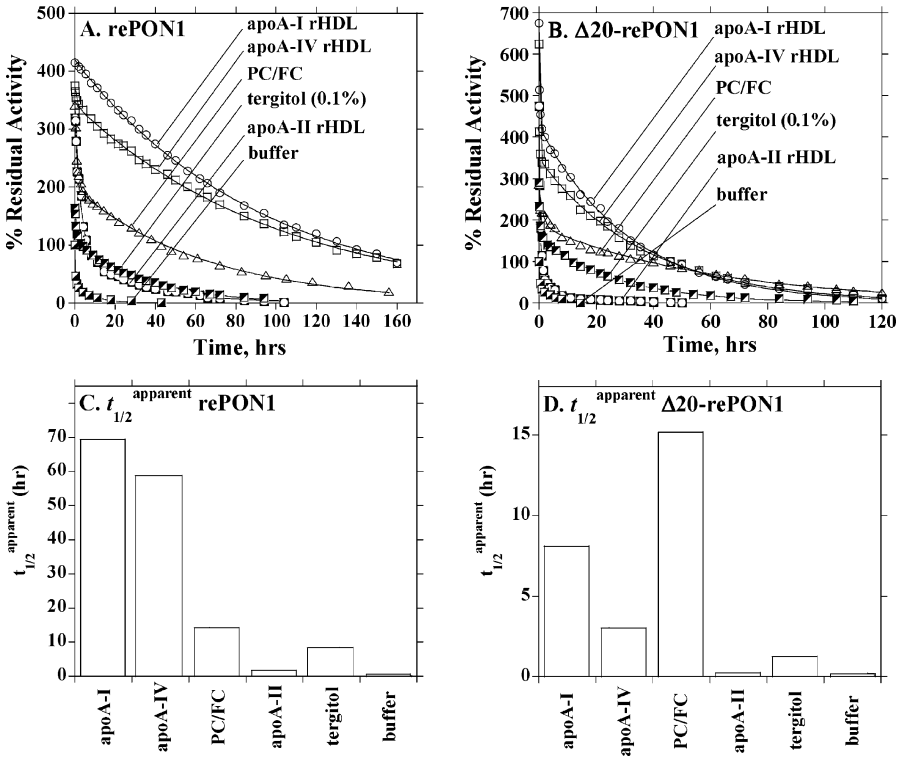

FIGURE 2: Kinetics of the inactivation of rePON1s in the solutions of various rHDL particles, 0.1% tergitol, or activity buffer (A and B). Delipidated rePON1s (0.2 μM) were incubated with a large excess of rHDL (10 μM), 0.1% tergitol (ca. 15 μM detergent micelles), or activity buffer and subjected to inactivation by EDTA (5 mM) and β-mercaptoethanol (10 mM) at 37 °C. Aliquotes were taken at certain time points and diluted in activity buffer, and residual activity was detected with phenyl acetate (1 mM). The initial activity of the delipidated enzyme in buffer corresponds to 100%. Data were fitted to a monoexponential function for rePON1 in an apoA-I rHDL solution, and to a double-exponential function for all the rest. Apparent half-lives ($t_{1/2}^{apparent}$) were derived from the curves and are plotted as bar graphs (C and D).

Table 2: Kinetic and Equilibrium Constants for the Inactivation of rePON1 and Δ20-rePON1 by EDTA and β-Mercaptoethanol[a]

	rePON1				Δ20-rePON1			
	A_1[b] (fast phase)	$k_1^{inactiv}$ (h^{-1})	A_2[b] (slow phase)	$k_2^{inactiv}$ (h^{-1})	A_1 (fast phase)	$k_1^{inactiv}$ (h^{-1})	A_2 (slow phase)	$k_2^{inactiv}$ (h^{-1})
apoA-I rHDL[c]	0	–	1.0	0.01	0.36	5.5	0.64	0.03
apoA-IV rHDL[c]	0.1	1.1	0.9	0.01	0.45	5.7	0.55	0.03
PC/FC[c]	0.42	0.9	0.58	0.01	0.32	1.3	0.68	0.02
apoA-II rHDL[c]	0.68	0.4	0.32	0.03	0.76	3.5	0.24	0.1
tergitol[c]	0.35	1.2	0.65	0.03	0.47	2.5	0.53	0.04
activity buffer[c]	0.7	3.1	0.3	0.2	0.5	3.3	0.5	0.2

[a] Amplitudes (A) and kinetic rates of inactivation ($k^{inactiv}$) were derived by fitting the data to an exponential curve: monoexponential, in the case of rePON1 interacting with apoA-I rHDL, and double exponential for all the rest. Subscripts 1 and 2 designate the first (fast) and the second (slow) phases of the inactivation, respectively. Each value represents the mean of two independent experiments. Standard deviations were less then 10% of parameter values. [b] Amplitudes of the first (A_1) and second (A_2) phases of the inactivation are represented as the fractional values of the total amplitude ($A_1 + A_2$). These values correspond to the equilibrium constant for the partitioning between the aqueous (unbound) and lipid-bound phases. [c] All the rHDLs were prepared by cholate dialysis and contained PC, FC, and the respective apolipoprotein (no apolipoprotein in the case of PC/FC). The tergitol solution was 0.1% in activity buffer [50 mM Tris (pH 8.0) and 1 mM $CaCl_2$]. Activity buffer samples were delipidated as described in Materials and Methods.

The apoA-II-anchored PON1 shows not only the highest fraction of the fast phase (0.68; similar to that for the delipidated sample) but also a higher rate of the slow phase ($k_2^{inactiv} = 0.03\ s^{-1}$). Overall, PON1 anchoring onto apoA-I rHDL had dramatic effects on the enzyme's activity and stability, leading to a >4-fold increase in arylesterase activity and a 350-fold increase in stability of the lipid-poor enzyme ($t_{1/2}^{apparent}$ values of ~70 and 0.2 h for PON1 in apoA-I rHDL mixture and buffer, respectively) (Figure 2C).

In contrast to the intact rePON1, the truncated enzyme exhibited two conformations with all the rHDL particles (Figure 2B), and displayed increased (up to 10-fold) inactivation rates for both the first (fast) and second (slow) phase (Table 2). Overall, anchoring of the truncated PON1 to apoA-I rHDL increased the stability by a factor of 40 (Figure 2D). Interestingly, the PC/FC vesicles have a stronger effect on the stability of Δ20-rePON1 than apoA-I and apoA-IV particles, indicating the importance of the N-terminus for the interaction with apolipoproteins on HDL.

Enzymatic Activity Measurements. We examined the effect of various HDL preparations on the enzymatic activity of rePONs. Delipidated enzymes were incubated with rHDL particles over a range of HDL concentrations (corresponding to a HDL/PON ratio of 0.5−50), and the catalytic activity was measured with various substrates at 1 mM ($\geq K_M$ values for all these substrates). Figure 3 shows the outcome of

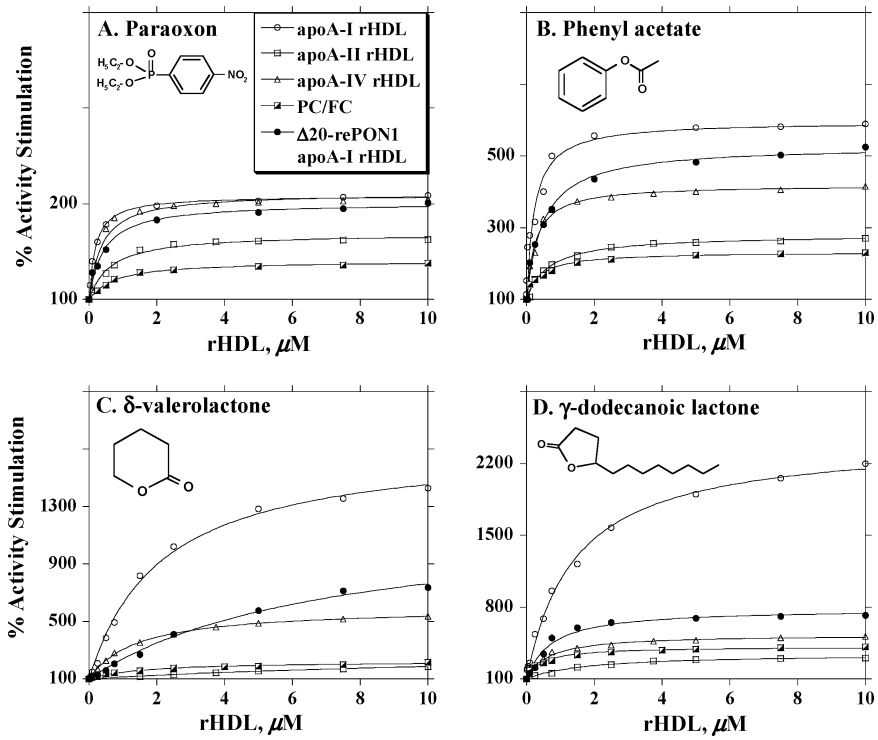

FIGURE 3: Stimulation of the enzymatic activity of rePON1 by different types of rHDLs (note the scale differences in the graphs). Delipidated rePON1, or Δ20-rePON1, was incubated with increasing concentrations of rHDLs (rHDL/rePON molar ratios of 0.5−50), and activity was tested with paraoxon (A), phenyl acetate (B), δ-valerolactone (C), and γ-dodecanoic lactone (D) (each substrate at 1 mM). All graphs refer to rePON1 interacting with apoA-I, apoA-II, apoA-IV, and PC/FC rHDLs, and Δ20-rePON1 interacting with apoA-I rHDL; annotations are the same for all the graphs. Stimulated activity is presented as the percentage of the initial activity of the delipidated enzyme. Data were fitted to the Langmuir saturation curve [$V = V_{max}$[rHDL]/([rHDL] + K_{app}) + 100]. Each curve represents an average of at least two experiments. The concentration of rHDL was determined on the basis of the apolipoprotein concentration, assuming an apoA/rHDL ratio of 2/1.

titration of rePONs by rHDLs for four substrates: paraoxon, phenyl acetate, and two lactones (δ-valerolactone and the hydrophobic γ-dodecanoic lactone). In accordance with previous observations (*19*, *27*), PON1 association with HDL led to a modest stimulation of the enzymatic activity with paraoxon and phenyl acetate. The stimulatory effect of the different rHDL preparations was very similar, as well as the increase in the activity of the intact versus truncated rePON1. The paraoxonase activity of rePON1 interacting with apoA-I rHDL increased by a factor of 2 relative to the initial activity of the delipidated enzyme. The same effect was observed with apoA-IV particles, while apoA-II rHDL and PC/FC particles led to a slightly smaller stimulatory effect (Figure 3A). The arylesterase activity exhibited an ∼6-fold stimulation with apoA-I rHDL, while the activity of rePON1 interacting with apoA-IV, apoA-II, and PC/FC particles increased by 2.5−4-fold (Figure 3B).

Interestingly, the effect of HDL binding on PON1's lactonase activity, which has not been examined before, is more dramatic and highly specific to apoA-I. Thus, rePON1 treated with apoA-I rHDL exhibited a 15-fold increased activity with δ-valerolactone and a >20-fold increased activity with γ-dodecanoic lactone (Figure 3C,D). Dihydrocoumarin, however, displayed a very mild stimulatory effect of 2-fold only (not shown), suggesting that it behaves differently in comparison to the above lactone substrates. Other HDL particles led to significantly lower stimulatory effects (2−5-fold). The Δ20-rePON1 treated with apoA-I rHDL exhibited an only 7-fold increased activity in accordance with its decreased affinity. This also is in contrast to the paraoxonase and arylesterase activities that are stimulated to a similar degree in both intact and truncated PON1.

The enzymatic activation data were fit to a Langmuir isotherm to give V_{max} values (in percent relative to the delipidated PON1) and K_{app} (concentration of HDL particles required for 50% stimulation) reflecting the activation factor and the apparent affinity for each type of particle, respectively (Table 3). This analysis indicated that the hydrolytic activity of intact rePON1 toward the hydrophobic γ-dodecanoic lactone improves by a factor of >24 when all enzyme molecules are anchored onto apoA-I rHDL particles. Neither apoA-IV, apoA-II, nor PC/FC vesicles are able to lead to this level of stimulation, nor is the truncated enzyme activated to the same degree. Interestingly, there are also variations in K_{app}. Stimulation of rePON1 by apoA-I rHDL gave 10-fold lower K_{app} values for the weakly stimulated substrates (paraoxon and phenyl acetate; $K_{app} = 0.2$ μM) than for the lactones ($K_{app} \approx 2$ μM). Do these differences imply differences in affinity? Not necessarily. We believe that they result from having a heterogeneous population of apoA-I rHDL particles. The fraction of particles that can induce the fully activated enzyme form required for the lactone substrates is roughly 10%, and hence the 10-fold higher K_{app} value. Notably, stabilization of the enzyme may be mediated by the larger fraction of particles. However, the composition of these fractions remains unclear. The degree of stabilization of rePON1 at different apoA-I rHDL concentrations gave an isotherm similar to that of arylesterase activation (Figure 3B) with a K_{app} value of 0.3 μM (Figure 4).

The kinetic parameters for the hydrolysis of paraoxon, phenyl acetate, δ-valerolactone, γ-dodecanoic lactone, and

Table 3: Enzymatic Activation of rePON1s by rHDLs with Various Apolipoprotein Compositions[a]

	paraoxon[b]		phenyl acetate		δ-valerolactone		γ-dodecanoic lactone	
	K_{app} (μM)[c]	V_{max} (%)[d]	K_{app} (μM)	V_{max} (%)	K_{app} (μM)	V_{max} (%)	K_{app} (μM)	V_{max} (%)
rePON1−apoA-I rHDL	0.2 ± 0.01	209 ± 1	0.2 ± 0.1	596 ± 23	2.1 ± 0.2	1740 ± 48	1.4 ± 0.1	2440 ± 57
rePON1−apoA-IV rHDL	0.4 ± 0.1	211 ± 4	0.3 ± 0.03	419 ± 6	1.4 ± 0.1	597 ± 5	0.6 ± 0.1	533 ± 11
rePON1−PC/FC	0.8 ± 0.1	140 ± 1	0.4 ± 0.1	232 ± 4	1.7 ± 0.2	226 ± 5	0.5 ± 0.1	415 ± 8
rePON1−apoA-II rHDL	0.6 ± 0.1	169 ± 2	0.7 ± 0.1	281 ± 5	14.7 ± 2.5	312 ± 25	1.8 ± 0.3	346 ± 11
Δ20-rePON1−apoA-I rHDL	0.4 ± 0.1	201 ± 3	0.5 ± 0.1	529 ± 11	7.1 ± 1.1	1232 ± 91	0.7 ± 0.1	686 ± 29

[a] Data were fitted to the Langmuir saturation curve, from which the K_{app} and V_{max} were directly derived. All values represent the derived parameters with the standard error of the fit. [b] All substrates were taken at 1 mM. [c] The apparent affinity for HDL stimulation is the concentration of rHDL that resulted in half-maximal stimulation of the activity. [d] V_{max} values are presented as the percentage relative to the delipidated enzyme.

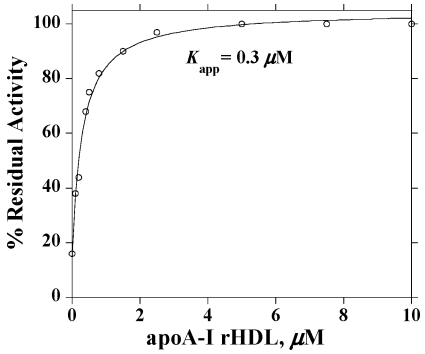

FIGURE 4: Stabilization of rePON1 at different apoA-I rHDL concentrations. Delipidated rePON1 (0.2 μM) was preincubated with a series of apoA-I rHDL concentrations and subjected to inactivation by EDTA (5 mM) and β-mercaptoethanol (10 mM) at 37 °C for 1 h. Residual activity was measured with phenyl acetate (1 mM) and expressed as the percentage of the initial activity at each HDL concentration. Data were fitted to the Langmuir saturation curve, yielding a K_{app} of 0.3 μM.

5-HETEL were determined, for rePON1 with apoA-I rHDL, micellar detergent (0.1% tergitol), or buffer (Table 4). PON1's catalytic activity (k_{cat}/K_M) is increased by ~2-fold with all the substrates in the presence of tergitol. Similar effects were observed for paraoxon and phenyl acetate when the enzyme was treated with apoA-I rHDL, while the activity with δ-valerolactone and γ-dodecanoic lactone increased by 14−18-fold, because of an increase in k_{cat} and a decrease in K_M. The affinity of rePON1 for γ-dodecanoic lactone is lower than that previously reported (*13*), probably due to the incomplete solubility of γ-dodecanoic lactone in the absence of Triton detergent, which was omitted since it might cause the dissociation of rePON1 from HDL. The increases in the catalytic efficiency of the enzyme in the presence of apoA-I rHDL correlate with the V_{max} values derived from the titration experiment (Table 3), although the lactonase activity did not reach the maximal stimulation level (as indicated in Table 4) because of the high K_{app} of rePON1 for rHDL. Nevertheless, the lactonase k_{cat}/K_M values of PON1 bound to apoA-I rHDL are $>10^6$ M^{-1} s^{-1}, and the turnover numbers (k_{cat}) are >600 s^{-1}. Moreover, using an HPLC assay, we tested the activity of PON1 bound to apoA-I rHDL toward 5-HETE lactone, an endogenous product of arachidonic acid oxidation shown to be a PON1 substrate (*10*). The k_{cat}/K_M reaches 1.5 × 10^7 M^{-1} s^{-1}, while the K_M appears to be in the low micromolar range. These values are characteristic of highly efficient enzymes acting on their native or physiological substrate (*39*).

DISCUSSION

Application of Recombinant PON1. In contrast to previous studies that were performed primarily with serum-purified human PON1, this study makes use of a recombinant PON1 variant generated by directed evolution for bacterial expression (*33*). The application of a reconstituted in vitro system based entirely on proteins expressed in *E. coli* provided a mean of preventing contamination by copurified serum components that can lead to conflicting results (*10*, *30*−*32*). One would need to make sure, however, that the recombinant PON1 reproduces the properties of native PON1. The variant applied here (G3C9) is a very close homologue of wild-type rabbit PON1 (95% amino acid identity and 98% similarity) and, in detergent micellar solution, was shown to possess enzymatic properties identical to those of rabbit as well as human PON1 with a wide range of substrates (*12*, *33*). The results presented here suggest that this rePON1 variant also maintains the HDL binding properties of native PON1. All the data presented here are novel, apart from the HDL-

Table 4: Enzymatic Parameters for rePON1 with ApoA-I rHDL, Micellar Detergent, or Buffer[a]

	activity buffer			tergitol (0.1%)			apoA-I rHDL		
	k_{cat} (s^{-1})	K_M (mM)	k_{cat}/K_M (M^{-1} s^{-1})	k_{cat} (s^{-1})	K_M (mM)	k_{cat}/K_M (M^{-1} s^{-1})	k_{cat} (s^{-1})	K_M (mM)	k_{cat}/K_M (M^{-1} s^{-1})
paraoxon	3.3 ± 0.3	0.9 ± 0.1	(3.7 ± 0.3) × 10^3 (**1**)[b]	5.8 ± 1.1	0.9 ± 0.2	(6.4 ± 0.1) × 10^3 (**2**)[b]	3.7 ± 0.2	0.5 ± 0.1	(7.4 ± 0.2) × 10^3 (**2**)[b]
phenyl acetate	509 ± 44	2.6 ± 0.8	(2.0 ± 0.5) × 10^5 (**1**)[b]	645 ± 21	1.6 ± 0.6	(5.6 ± 1.0) × 10^5 (**3**)[b]	685 ± 93	0.8 ± 0.1	(8.6 ± 0.7) × 10^5 (**4**)[b]
δ-valerolactone	94 ± 20	1.0 ± 0.1	(0.9 ± 0.3) × 10^5 (**1**)[b]	156 ± 10	0.9 ± 0.1	(1.7 ± 0.1) × 10^5 (**2**)[b]	632 ± 16	0.5 ± 0.1	(1.3 ± 0.1) × 10^6 (**14**)[b]
γ-dodecanoic lactone[c]	nd[d]	nd[d]	(2.2 ± 0.2) × 10^4 (**1**)[b]	34 ± 4	0.7 ± 0.1	(4.9 ± 0.4) × 10^4 (**2**)[b]	101 ± 1	0.3 ± 0.1	(3.9 ± 0.7) × 10^5 (**18**)[b]
5-HETEL	nd[d]	nd[d]	(1.7 ± 0.3) × 10^6 (**1**)[b]	nd[d]	nd[d]	(4.6 ± 1) × 10^6 (**3**)[b]	nd[d]	nd[d]	(1.5 ± 0.3) × 10^7 (**9**)[b]

[a] Delipidated rePON1 (0.2 μM) in activity buffer was incubated with 0.1% tergitol or apoA-I rHDL (10 μM) and subjected to Michaelis−Menten kinetic analysis. Each value represents the mean ± the standard deviation of two experiments. [b] Bold numbers show the *x*-fold improvement of k_{cat}/K_M relative to that of the delipidated enzyme in activity buffer. [c] γ-Dodecanoic lactone requires addition of detergent due to the low solubility in buffer (*13*). However, the detergent was omitted since it might cause the dissociation of rePON1 from HDL. [d] Not determined.

Table 5: Correlation of Affinity, Stability, and Lactonase Activity of PON1 on Various HDL Particles

	rePON1				Δ20-rePON1			
	K_d (M)[a]	A_{slow}/A_{fast}[b]	$t_{1/2}^{apparent}$ (h)[c]	V_{max} (%)[d]	K_d (M)[a]	A_{slow}/A_{fast}[b]	$t_{1/2}^{apparent}$ (h)[c]	V_{max} (%)[d]
apoA-I rHDL	$<0.75 \times 10^{-9}$	≥ 100	69	2440	1.2×10^{-7}	2	8	686
apoA-IV rHDL	$\leq 1.3 \times 10^{-9}$	9	59	533	1.6×10^{-7}	1	3	nd[e]
PC/FC	$\leq 3.2 \times 10^{-9}$	1	14	415	5.9×10^{-8}	2	15	367
apoA-II rHDL	$\leq 4.4 \times 10^{-8}$	0.5	2	346	1.8×10^{-6}	0.3	0.2	nd[e]

[a] Affinity constants (K_d) were obtained from the BIAcore binding experiments (Table 1). [b] Partition coefficients of rePON1s between the lipid and aqueous phase (A_{slow}/A_{fast}) were derived from the stability measurements (Table 2). A_{slow} and A_{fast} stand for A_2 and A_1, respectively. [c] Apparent half-lives ($t_{1/2}^{apparent}$) were derived from the stability measurements (Figure 2C,D). [d] Stimulation factors with γ-dodecanoic lactone (V_{max}) were derived from the analysis of enzymatic activation of rePON1s by rHDLs (Table 3). [e] Not determined.

mediated stimulation of PON1's arylesterase activity (Figure 3B). This has been examined before with human PON1 and both native (*19*) and rHDL (*18*, *19*, *27*) particles, and yielded essentially identical stimulation patterns, in terms of both V_{max} (activation factors) and K_{app}. In fact, the resemblance of rePON1 G3C9 to native PON1 is not surprising, considering that most of the amino acid substitutions acquired in the course of laboratory evolution are located in buried regions of the protein (*40*). In addition, it appears that glycosylation is not essential for the enzymatic activity of PON1 (*10*, *33*), or for the anchoring of the enzyme onto HDL, as expected from the location of PON1's glycosylation sites that appear to be distant from the HDL's surface (*14*). Thus, the bacterially expressed rePON1 variant used in this study appears to preserve both the enzymatic properties of native PON1 and its HDL binding properties, thus making it a useful tool in the mechanistic and structural studies of PON1.

Correlating Affinity, Stability, and Lactonase Activity. A remarkable correlation was observed between the affinity, the stability, and the enzymatic activity of PON1 on various HDL particles. Taken together with the affinity measurements, the first (fast) and second (slow) phases of the inactivation reaction (A_1 and A_2, respectively) appear to correspond to the solution (unbound) and HDL-bound PON1 molecules, respectively. Assuming that the lipid- or HDL-bound form is the more stable one, the ratio of these amplitudes provides a measure of the partition coefficient of the enzyme between the lipid particles (or detergent micelles) and the aqueous phase. Table 5 shows a comparison of the ratio between the amplitudes of the slow and fast phase of the inactivation kinetics (A_{slow}/A_{fast}), with the dissociation constants (K_d) of PON1 for different rHDL particles. The two parameters correlate for both intact and truncated rePON1. The marked difference between apoA-I ($A_{slow}/A_{fast} \geq 100$) and apoA-IV ($A_{slow}/A_{fast} = 9$) supports our assumption that the affinity of PON1 for apoA-I rHDL is significantly higher than our estimate ($K_d < 0.75 \times 10^{-9}$ M). A marked difference between apoA-I and apoA-IV was also observed with the level of lactonase activity (Figure 3C,D).

Altogether, the stability and lactonase activity of the HDL-anchored PON1 correlate very well with its affinity toward these particles (Table 5). By virtue of the high binding affinity ($K_d \ll 10^{-9}$ M), apoA-I rHDL particles induce a single, highly stable, and active conformation of PON1. ApoA-IV appears to have similar although lower capability, and significantly lower affinity. ApoA-II has a marked negative effect; the affinity, stability, and enzymatic activity of PON1 are dramatically reduced relative to those of lipopoprotein-free particles (PC/FC vesicles). The latter clearly provide a better environment than detergent micelles, the affinity of which for PON1 is presumably in the upper micromolar range.

PON1's Association with Different HDL Particles. PON1 possesses a very high affinity for apoA-I rHDL ($K_d \ll 10^{-9}$ M), and very slow dissociation kinetics (half-life of >80 min). For comparison, binding of another HDL-associated enzyme, lecithin cholesterol acyl transferase (LCAT), to apoA-I rHDL proceeds with a >100-fold lower affinity, and its dissociation rate is >80 times faster (*37*). While apoA-IV and PC/FC particles still bind PON1 with nanomolar affinities, apoA-II particles displayed a decrease in affinity of ca. 100-fold, reduced stability, and enzymatic activity. These findings account for previous ex vivo experiments, in which apoA-I rHDL was shown to act as an optimal PON1 acceptor, although phospholipid vesicles could also promote PON1 release (*18*, *19*, *26*). In vivo studies showed that apoA-I deficiencies (*41*, *42*), as well as apoA-I knockout mice (*18*, *43*), are characterized by lower PON1 levels. Further, PON1 activity in the apoA-I deficient mice was associated with the VHDL fractions that contain, among other apolipoproteins, apoA-IV (*44*, *45*), suggesting that these particles can act as secondary PON1 carriers (*46*).

Ex vivo studies reported different observations regarding PON1 association with apoA-II-containing HDL: on one hand, apoA-II particles could promote PON1 secretion and stabilize the enzyme (*19*), but on the other hand, there was a loss of PON1 activity from apoA-II vesicles (*18*). In vivo studies, however, consistently indicate the detrimental effect of apoA-II on the PON1 content of HDL that is in agreement with the dramatically reduced affinity, stability, and lactonase activity observed here. ApoA-II transgenic mice exhibited a substantial reduction in serum PON1 levels and specific activity, including the loss of the ability to inhibit LDL oxidation (*47*−*50*). The negative effects of apoA-II might be related to several factors, including the highly hydrophobic nature of apoA-II and the size of HDL particles. ApoA-II readily displaces apoA-I from native and reconstituted HDL (*51*−*53*), and becomes associated with smaller HDL complexes (*54*, *55*). Smaller HDL particles were shown to be less efficient PON1 acceptors (*19*). Formation of apoA-II particles from apoA-I HDL influences the function of the most important enzymes in HDL metabolism, leading to inactivation of LCAT (*55*), inhibition or activation of hepatic lipase (*56*), and inhibition of LDL−HDL lipid exchange mediated by phospholipid transfer protein (*57*). Given the above, it is tempting to speculate that apoA-II competes for the hydrophobic sites of HDL, thus preventing the association of PON1 with the lipoprotein.

PON1's Mode of Binding to HDL. The affinity of N-terminally truncated PON1 (Δ20-rePON1) is ≥ 100 fold

lower compared to that of the intact protein, for all rHDL particles almost regardless of their protein component (Table 1). This observation supports the established role of PON1's N-terminal helix in association with lipoproteins (*18*). Moreover, the highest affinity and stability of the truncated PON1 were observed with PC/FC vesicles devoid of any apolipoprotein, probably indicating the involvement of the N-terminus in the interaction with apolipoproteins on HDL. However, the affinity of the truncated PON1 is comparatively high and very similar to that of LCAT (the K_d for apoA-I rHDL is 1.2×10^{-7} M), suggesting the role of additional parts of PON1. Indeed, the crystal structure of PON1 indicated the existence of an amphipatic helix (H2) in the vicinity of the N-terminal helix (H1) and PON1's active site (*14*), which could be involved in HDL binding. In fact, H2 comprises part of the active site wall, and the model suggests that the top of the active site is partly covered by the HDL surface. One of the active site loops is disordered and hence not seen in the structure (residues 72−79), and may comprise an active site lid. While the detailed mode of binding is yet to be resolved, it appears that PON1 exhibits some distinct features of an interfacially activated enzyme. Interestingly, the presence of the transmembrane helix that reinforces membrane binding mediated by hydrophobic elements surrounding the active site entrance (e.g., H2) is a common characteristic of unconventional integral membrane proteins, suggesting a modular adaptation of soluble proteins that directs them to the membrane surface (*58*).

Stabilization of PON1 by HDL. Previous reports on PON1's interaction with HDL indicated the increased stability of enzyme samples in the presence of the lipoproteins (*18*, *19*) and a significant decrease in the levels of serum PON1 in apoA-I deficiency diseases (*41*, *42*). Our results confirm that PON1's stability depends on its lipidation state, and provide a quantitative description of at least two distinct forms of PON1. In a micellar solution of various amphiphiles (be they lipoproteins or detergents), PON1 exists in two distinct forms: stable ($t_{1/2}^{inact} \sim 70$ h) and unstable ($t_{1/2}^{inact} \sim 0.7$ h). Amphiphilic molecules of various types shift the equilibrium toward the stable form. Further, the relative distribution of the two forms is directly related to the affinity of PON1 for the lipoprotein complexes, and only apoA-I rHDL, which exhibits the highest affinity (Table 5), is capable of totally shifting the equilibrium in favor of the stable form. Analysis of the oligomeric states of PON1 indicated that, in detergent-free solutions, PON1 formed multiple aggregates of two to four molecules while, in micellar detergent solutions, a reversible monomer−dimer equilibrium was observed (*20*). Nondenaturing gel electrophoresis and zymograms of lipid-poor, and HDL-associated, PON1 supported this model by indicating the disappearance of PON1 oligomers in the presence of the apoA-I rHDL (data not shown). It appears that the stable and unstable forms of PON1 might in fact correspond to the different oligomeric states of lipid-bound and lipid-poor PON1.

ApoA-I HDL Selectively Stimulates the Lactonase Activity of PON1. Preincubation of purified human serum PON1 with phospholipids has been long known to stimulate its hydrolytic activity toward paraoxon, aryl esters, and lactones (*2*, *38*, *59*), and was recently shown to stimulate the lactonization activity of PON1, as well (*11*). These stimulation effects, however, were quite modest (≤2-fold). Other studies indicated that HDL stimulates PON1's arylesterase activity by a factor of ∼5 (*18*, *19*, *27*). Here, we extended these studies to examine the selectivity of the catalytic stimulation and the role played by different lipid and protein components. Our results indicate unequivocally that apoA-I HDL has a unique ability to stimulate the lactonase activity of PON1, an activity that is now deemed PON1's native activity (*10*, *13*). The specific lactonase stimulation effect was not observed with other apolipoproteins, phospholipid vesicles, or detergent micelles, which activate all activities (paraoxonase, arylesterase, and lactonase) to a similar degree. The N-terminus of PON1 does not seem to be directly involved in the stimulation process, as the lactonase activity of the truncated variant (Δ20-rePON1) is also stimulated by apoA-I HDL, although to a lower degree than the intact enzyme in accordance to the decreased HDL affinity.

CONCLUSIONS

This study shows that dramatic changes in the biochemical and enzymatic properties of PON1 take place upon its association with HDL. Apolipoprotein A-I appears to play an important role in this interaction by generating lipoprotein particles with an unexpectedly high affinity for PON1 and inducing a single, highly stable, and active conformation of the enzyme. Altogether, it appears that PON1 is a highly proficient, interfacially activated lactonase. Moreover, our structural and biochemical studies of PON1 suggest that it belongs to the newly emerging family of unconventional integral membrane proteins (IMPs) (*58*). These enzymes adhere to the membrane bilayer through variable structural elements, and gain access to their hydrophobic substrates by the intimate relationship between the membrane-binding domain and active site. Future studies will elucidate whether the interfacial effects are mediated through direct interaction of apoA-I with PON1, and which molecular elements of both proteins are involved in this interaction.

ACKNOWLEDGMENT

We are very thankful to Dr. Michael Oda (Oakland Research Institute) and Kevin Pearson and Dr. Sean Davidson (University of Cincinnati) for providing human apoA-I and apoA-IV plasmids, respectively, as well as important technical support. We are also grateful to Erick Alexander (Wake Forest University, Winston-Salem, NC), Dr. Lihua Jin (DePaul University, Chicago, IL), and Dr. Dragomir Draganov (The University of Michigan, Ann Arbor, MI) for providing protocols for the preparation of reconstituted HDL, Biacore analysis, and the HPLC lactonase assay, respectively.

REFERENCES

1. Draganov, D. I., and La Du, B. N. (2004) Pharmacogenetics of paraoxonases: A brief review, *Naunyn-Schmiedeberg's Arch. Pharmacol. 369*, 78−88.
2. Billecke, S., Draganov, D., Counsell, R., Stetson, P., Watson, C., Hsu, C., and La Du, B. N. (2000) Human serum paraoxonase (PON1) isozymes Q and R hydrolyze lactones and cyclic carbonate esters, *Drug Metab. Dispos. 28*, 1335−1342.
3. Durrington, P. N., Mackness, B., and Mackness, M. I. (2001) Paraoxonase and atherosclerosis, *Arterioscler. Thromb. Vasc. Biol. 21*, 473−480.
4. Costa, L. G., Cole, T. B., Jarvik, G. P., and Furlong, C. E. (2003) Functional genomic of the paraoxonase (PON1) polymorphisms: Effects on pesticide sensitivity, cardiovascular disease, and drug metabolism, *Annu. Rev. Med. 54*, 371−392.

5. Shih, D. M., Gu, L., Xia, Y. R., Navab, M., Li, W. F., Hama, S., Castellani, L. W., Furlong, C. E., Costa, L. G., Fogelman, A. M., and Lusis, A. J. (1998) Mice lacking serum paraoxonase are susceptible to organophosphate toxicity and atherosclerosis, *Nature 394*, 284−287.
6. Bowry, V. W., Stanley, K. K., and Stocker, R. (1992) High-density lipoprotein is the major carrier of lipid hydroperoxides in human blood plasma from fasting donors, *Proc. Natl. Acad. Sci. U.S.A. 89*, 10316−10320.
7. Lusis, A. J. (2000) Atherosclerosis, *Nature 407*, 233−241.
8. Ahmed, Z., Ravandi, A., Maguire, G. F., Emili, A., Draganov, D., La Du, B. N., Kuksis, A., and Connelly, P. W. (2001) Apolipoprotein A-I promotes the formation of phosphatidylcholine core aldehydes that are hydrolyzed by paraoxonase (PON-1) during high-density lipoprotein oxidation with a peroxynitrite donor, *J. Biol. Chem. 276*, 24473−24481.
9. Aviram, M., Hardak, E., Vaya, J., Mahmood, S., Milo, S., Hoffman, A., Billicke, S., Draganov, D., and Rosenblat, M. (2000) Human serum paraoxonases (PON1) Q and R selectively decrease lipid peroxides in human coronary and carotid atherosclerotic lesions: PON1 esterase and peroxidase-like activities, *Circulation 101*, 2510−2517.
10. Draganov, D. I., Teiber, J. F., Speelman, A., Osawa, Y., Sunahara, R., and La Du, B. N. (2005) Human paraoxonases (PON1, PON2, and PON3) are lactonases with overlapping and distinct substrate specificities, *J. Lipid Res. 46*, 1239−1247.
11. Teiber, J. F., Draganov, D. I., and La Du, B. N. (2003) Lactonase and lactonizing activities of human serum paraoxonase (PON1) and rabbit serum PON3, *Biochem. Pharmacol. 66*, 887−896.
12. Aharoni, A., Gaidukov, L., Khersonsky, O., Mc, Q. G. S., Roodveldt, C., and Tawfik, D. S. (2005) The 'evolvability' of promiscuous protein functions, *Nat. Genet. 37*, 73−76.
13. Khersonsky, O., and Tawfik, D. S. (2005) Structure−Reactivity Studies of Serum Paraoxonase PON1 Suggest that Its Native Activity Is Lactonase, *Biochemistry 44*, 6371−6382.
14. Harel, M., Aharoni, A., Gaidukov, L., Brumshtein, B., Khersonsky, O., Meged, R., Dvir, H., Ravelli, R. B., McCarthy, A., Toker, L., Silman, I., Sussman, J. L., and Tawfik, D. S. (2004) Structure and evolution of the serum paraoxonase family of detoxifying and anti-atherosclerotic enzymes, *Nat. Struct. Mol. Biol. 11*, 412−419.
15. Adams, T. B., Greer, D. B., Doull, J., Munro, I. C., Newberne, P., Portoghese, P. S., Smith, R. L., Wagner, B. M., Weil, C. S., Woods, L. A., and Ford, R. A. (1998) The FEMA GRAS assessment of lactones used as a flavour ingredients. The Flavor and Extract Manufacturers' Association. Generally recognized as safe, *Food Chem. Toxicol. 36*, 249−278.
16. Mackness, M. I., Mackness, B., Durrington, P. N., Connelly, P. W., and Hegele, R. A. (1996) Paraoxonase: Biochemistry, genetics and relationship to plasma lipoproteins, *Curr. Opin. Lipidol. 7*, 69−76.
17. Navab, M., Hama, S. Y., Hough, G. P., Hedrick, C. C., Sorenson, R., La Du, B. N., Kobashigawa, J. A., Fonarow, G. C., Berliner, J. A., Laks, H., and Fogelman, A. M. (1998) High-density associated enzymes: Their role in vascular biology, *Curr. Opin. Lipidol. 9*, 449−456.
18. Sorenson, R. C., Bisgaier, C. L., Aviram, M., Hsu, C., Billecke, S., and La Du, B. N. (1999) Human serum Paraoxonase/Arylesterase's retained hydrophobic N-terminal leader sequence associates with HDLs by binding phospholipids: Apolipoprotein A-I stabilizes activity, *Arterioscler. Thromb. Vasc. Biol. 19*, 2214−2225.
19. Deakin, S., Leviev, I., Gomaraschi, M., Calabresi, L., Franceschini, G., and James, R. W. (2002) Enzymatically active paraoxonase-1 is located at the external membrane of producing cells and released by a high affinity, saturable, desorption mechanism, *J. Biol. Chem. 277*, 4301−4308.
20. Josse, D., Ebel, C., Stroebel, D., Fontaine, A., Borges, F., Echalier, A., Baud, D., Renault, F., Le Maire, M., Chabrieres, E., and Masson, P. (2002) Oligomeric states of the detergent-solubilized human serum paraoxonase (PON1), *J. Biol. Chem. 277*, 33386−33397.
21. Hassett, C., Richter, R. J., Humbert, R., Chapline, C., Crabb, J. W., Omiecinski, C. J., and Furlong, C. E. (1991) Characterization of cDNA clones encoding rabbit and human serum paraoxonase: The mature protein retains its signal sequence, *Biochemistry 30*, 10141−10149.
22. Lund-Katz, S., Liu, L., Thuahnai, S. T., and Phillips, M. C. (2003) High-density lipoprotein structure, *Front. Biosci. 8*, d1044−d1054.
23. Marcel, Y. L., and Kiss, R. S. (2003) Structure−function relationships of apolipoprotein A-I: A flexible protein with dynamic lipid associations, *Curr. Opin. Lipidol. 14*, 151−157.
24. Segrest, J. P., Harvey, S. C., and Zannis, V. (2000) Detailed molecular model of apolipoprotein A-I on the surface of high-density lipoproteins and its functional implications, *Trends Cardiovasc. Med. 10*, 246−252.
25. James, R. W., Hochstrasser, D., Tissot, J. D., Funk, M., Appel, R., Barja, F., Pellegrini, C., Muller, A. F., and Pometta, D. (1988) Protein heterogeneity of lipoprotein particles containing apolipoprotein A-I without apolipoprotein A-II and apolipoprotein A-I with apolipoprotein A-II isolated from human plasma, *J. Lipid Res. 29*, 1557−1571.
26. James, R. W., and Deakin, S. P. (2004) The importance of high-density lipoproteins for paraoxonase-1 secretion, stability, and activity, *Free Radical Biol. Med. 37*, 1986−1994.
27. Oda, M. N., Bielicki, J. K., Berger, T., and Forte, T. M. (2001) Cysteine substitutions in apolipoprotein A-I primary structure modulate paraoxonase activity, *Biochemistry 40*, 1710−1718.
28. Gan, K. N., Smolen, A., Eckerson, H. W., and La Du, B. N. (1991) Purification of human serum paraoxonase/arylesterase. Evidence for one esterase catalyzing both activities, *Drug Metab. Dispos. 19*, 100−106.
29. Blatter, M. C., James, R. W., Messmer, S., Barja, F., and Pometta, D. (1993) Identification of a distinct human high-density lipoprotein subspecies defined by a lipoprotein-associated protein, K-45. Identity of K-45 with paraoxonase, *Eur. J. Biochem. 211*, 871−879.
30. Marathe, G. K., Zimmerman, G. A., and McIntyre, T. M. (2003) Platelet-activating factor acetylhydrolase, and not paraoxonase-1, is the oxidized phospholipid hydrolase of high-density lipoprotein particles, *J. Biol. Chem. 278*, 3937−3947.
31. Fokine, A., Morales, R., Contreras-Martel, C., Carpentier, P., Renault, F., Rochu, D., and Chabriere, E. (2003) Direct phasing at low resolution of a protein copurified with human paraoxonase (PON1), *Acta Crystallogr. D59*, 2083−2087.
32. Connelly, P. W., Draganov, D., and Maguire, G. F. (2005) Paraoxonase-1 does not reduce or modify oxidation of phospholipids by peroxynitrite, *Free Radical Biol. Med. 38*, 164−174.
33. Aharoni, A., Gaidukov, L., Yagur, S., Toker, L., Silman, I., and Tawfik, D. S. (2004) Directed evolution of mammalian paraoxonases PON1 and PON3 for bacterial expression and catalytic specialization, *Proc. Natl. Acad. Sci. U.S.A. 101*, 482−487.
34. Pearson, K., Saito, H., Woods, S. C., Lund-Katz, S., Tso, P., Phillips, M. C., and Davidson, W. S. (2004) Structure of human apolipoprotein A-IV: A distinct domain architecture among exchangeable apolipoproteins with potential functional implications, *Biochemistry 43*, 10719−10729.
35. Nichols, A. V., Gong, E. L., Blanche, P. J., and Forte, T. M. (1983) Characterization of discoidal complexes of phosphatidylcholine, apolipoprotein A-I and cholesterol by gradient gel electrophoresis, *Biochim. Biophys. Acta 750*, 353−364.
36. Matz, C. E., and Jonas, A. (1982) Micellar complexes of human apolipoprotein A-I with phosphatidylcholines and cholesterol prepared from cholate-lipid dispersions, *J. Biol. Chem. 257*, 4535−4540.
37. Jin, L., Shieh, J. J., Grabbe, E., Adimoolam, S., Durbin, D., and Jonas, A. (1999) Surface plasmon resonance biosensor studies of human wild-type and mutant lecithin cholesterol acyltransferase interactions with lipoproteins, *Biochemistry 38*, 15659−15665.
38. Kuo, C. L., and La Du, B. N. (1995) Comparison of purified human and rabbit serum paraoxonases, *Drug Metab. Dispos. 23*, 935−944.
39. Fersht, A. (1999) *Structure and mechanism in protein science: A guide to enzyme catalysis and protein folding*, W. H. Freeman and Co., New York.
40. Roodveldt, C., Aharoni, A., and Tawfik, D. S. (2005) Directed evolution of proteins for heterologous expression and stability, *Curr. Opin. Struct. Biol. 15*, 50−56.
41. James, R. W., Blatter Garin, M. C., Calabresi, L., Miccoli, R., von Eckardstein, A., Tilly-Kiesi, M., Taskinen, M. R., Assmann, G., and Franceschini, G. (1998) Modulated serum activities and concentrations of paraoxonase in high-density lipoprotein deficiency states, *Atherosclerosis 139*, 77−82.
42. Mackness, M. I., Walker, C. H., and Carlson, L. A. (1987) Low A-esterase activity in serum of patients with fish-eye disease, *Clin. Chem. 33*, 587−588.
43. Cabana, V. G., Reardon, C. A., Feng, N., Neath, S., Lukens, J., and Getz, G. S. (2003) Serum paraoxonase: Effect of the

apolipoprotein composition of HDL and the acute phase response, *J. Lipid Res. 44*, 780−792.
44. Li, H., Reddick, R. L., and Maeda, N. (1993) Lack of apoA-I is not associated with increased susceptibility to atherosclerosis in mice, *Arterioscler. Thromb. 13*, 1814−1821.
45. Plump, A. S., Azrolan, N., Odaka, H., Wu, L., Jiang, X., Tall, A., Eisenberg, S., and Breslow, J. L. (1997) ApoA-I knockout mice: Characterization of HDL metabolism in homozygotes and identification of a post-RNA mechanism of apoA-I up-regulation in heterozygotes, *J. Lipid Res. 38*, 1033−1047.
46. Deakin, S., Moren, X., and James, R. W. (2005) Very low-density lipoproteins provide a vector for secretion of paraoxonase-1 from cells, *Atherosclerosis 179*, 17−25.
47. Warden, C. H., Hedrick, C. C., Qiao, J. H., Castellani, L. W., and Lusis, A. J. (1993) Atherosclerosis in transgenic mice overexpressing apolipoprotein A-II, *Science 261*, 469−472.
48. Castellani, L. W., Navab, M., Van Lenten, B. J., Hedrick, C. C., Hama, S. Y., Goto, A. M., Fogelman, A. M., and Lusis, A. J. (1997) Overexpression of apolipoprotein AII in transgenic mice converts high-density lipoproteins to proinflammatory particles, *J. Clin. Invest. 100*, 464−474.
49. Boisfer, E., Stengel, D., Pastier, D., Laplaud, P. M., Dousset, N., Ninio, E., and Kalopissis, A. D. (2002) Antioxidant properties of HDL in transgenic mice overexpressing human apolipoprotein A-II, *J. Lipid Res. 43*, 732−741.
50. Ribas, V., Sanchez-Quesada, J. L., Anton, R., Camacho, M., Julve, J., Escola-Gil, J. C., Vila, L., Ordonez-Llanos, J., and Blanco-Vaca, F. (2004) Human apolipoprotein A-II enrichment displaces paraoxonase from HDL and impairs its antioxidant properties: A new mechanism linking HDL protein composition and antiatherogenic potential, *Circ. Res. 95*, 789−797.
51. Edelstein, C., Halari, M., and Scanu, A. M. (1982) On the mechanism of the displacement of apolipoprotein A-I by apolipoprotein A-II from the high-density lipoprotein surface. Effect of concentration and molecular forms of apolipoprotein A-II, *J. Biol. Chem. 257*, 7189−7195.
52. Lopez, J., Latta, M., Collet, X., Vanloo, B., Jung, G., Denefle, P., Rosseneu, M., and Chambaz, J. (1994) Purification and characterization of recombinant human apolipoprotein A-II expressed in *Escherichia coli*, *Eur. J. Biochem. 225*, 1141−1150.
53. Mowri, H. O., Patsch, J. R., Gotto, A. M., Jr., and Patsch, W. (1996) Apolipoprotein A-II influences the substrate properties of human HDL2 and HDL3 for hepatic lipase, *Arterioscler. Thromb. Vasc. Biol. 16*, 755−762.
54. Rye, K. A. (1990) Interaction of apolipoprotein A-II with recombinant HDL containing egg phosphatidylcholine, unesterified cholesterol and apolipoprotein A-I, *Biochim. Biophys. Acta 1042*, 227−236.
55. Labeur, C., Lambert, G., Van Cauteren, T., Duverger, N., Vanloo, B., Chambaz, J., Vandekerckhove, J., Castro, G., and Rosseneu, M. (1998) Displacement of apo A-I from HDL by apo A-II or its C-terminal helix promotes the formation of pre-β1 migrating particles and decreases LCAT activation, *Atherosclerosis 139*, 351−362.
56. Jahn, C. E., Osborne, J. C., Jr., Schaefer, E. J., and Brewer, H. B., Jr. (1983) Activation of the enzymic activity of hepatic lipase by apolipoprotein A-II. Characterization of a major component of high-density lipoprotein as the activating plasma component in vitro, *Eur. J. Biochem. 131*, 25−29.
57. Pussinen, P. J., Jauhiainen, M., and Ehnholm, C. (1997) ApoA-II/apoA-I molar ratio in the HDL particle influences phospholipid transfer protein-mediated HDL interconversion, *J. Lipid Res. 38*, 12−21.
58. Bracey, M. H., Cravatt, B. F., and Stevens, R. C. (2004) Structural commonalities among integral membrane enzymes, *FEBS Lett. 567*, 159−165.
59. La Du, B. N., Adkins, S., Kuo, C. L., and Lipsig, D. (1993) Studies on human serum paraoxonase/arylesterase, *Chem.-Biol. Interact. 87*, 25−34.

BI050862I